Investigation on Caster Breakout During Flying Tundish Change and Separation Plate Using Innovative Techniques at ArcelorMittal Dofasco's No. 1 Continuous Caster



A caster breakout event occurred at ArcelorMittal Dofasco's No. 1 Continuous Caster in proximity to a grade transition with a flying tundish change and separator plate. Practices of flying tundish changes and separator plates have been well-established to cast grades of different chemistries with minimal interruption to productivity. Hence, it was unusual that a breakout occurred, well below the mold, despite these practices and this specific grade transition being successful multiple times prior. This article discusses innovative tools and techniques for the extensive investigation carried out and proposes an explanation of the breakout event, supported through evidence in the autopsy.

Authors

Jackie Leung (top left), Senior Researcher, ArcelorMittal Global R&D – Hamilton, Hamilton, Ont., Canada
jackie.leung@arcelormittal.com

Norbert Strobl (top right), Caster Technical Expert, ArcelorMittal Dofasco G.P., Hamilton, Ont., Canada
norbert.strobl@arcelormittal.com

Ali Mrad (bottom), Researcher, ArcelorMittal Global R&D – Hamilton, Hamilton, Ont., Canada
ali.mrad@arcelormittal.com

Introduction

ArcelorMittal Dofasco has two steel-producing streams (Fig. 1).[1] The KOBM stream uses one basic oxygen furnace where the tapped heats are refined at the ladle metallurgy facility (LMF 1) and cast at the No. 1 Continuous Caster (1CC); some grades are processed at the tank degasser (TDG) prior to casting. The electric arc furnace (EAF) stream uses a twin-shell EAF, where the tapped heats are refined at LMF 2 and cast at 2CC. A broad range of grades are produced between the two streams, which include: ultralow-carbon (ULC), low-carbon (LC), medium-carbon, high-carbon, high-strength low-alloy (HSLA), and advanced high-strength steel (AHSS).

Refractory components in the casting machine (e.g., submerged entry nozzle, ladle shroud, tundish lining) wear out over time and need to be replaced. Terminating the steel strand by halting casting ("sequence break"), replacing the tundish, and starting a new steel strand is time-consuming and results in lost productivity.[2] To optimize productivity, operators will execute a flying tundish change (FTC) to transition from the old tundish to a new tundish without terminating the steel strand. Because of ArcelorMittal Dofasco's diverse product mix, the scheduled heats for one tundish sequence may not be identical to the next.[3] As a result, grade mixing in the strand can occur affecting the final chemistry of the slabs. To limit the amount of grade mixing, operators will sometimes insert grade separator plate during an FTC depending on the grade transition.[4] This practice is identified at the casters as a tundish change-separator plate (TC-SP).[3] This practice is explained in greater detail by Leung and Trinh.[2]

Figure 1

ArcelorMittal Dofasco steelmaking process diagram.[1]

Figure 2

Breakout shell extracted from 1CC at mold (a); Segment 0 – Bender (Note: Photo is of a portion of the shell after it fractured) (b); and upper section of Segment 1 (c).

(a) (b) (c)

Unfortunately, a caster breakout occurred at 1CC, risking people and process safety and resulting in lost productivity. Fortunately, thanks to ArcelorMittal Dofasco safety procedures, the breakout did not lead to any injuries. The breakout occurred several minutes after a TC-SP which involved a grade transition from ULC to AHSS. There are inherent risks to mixing different grades, which include breakouts.[5] Nonetheless, this breakout event was rather unusual, as this practice occurs daily and has been well-established at 1CC to sequentially cast different grades with minimal interruption to productivity.[2–6] Furthermore, this specific grade transition had been successfully executed multiple times prior without any issues. A breakout autopsy was conducted on the slab and shell materials using some of the methodologies described by Leung and Sengupta,[7] as well as some new methods specific for this investigation. This article provides a brief description of the breakout event, the tools and techniques applied for this investigation, as well as an evidence-based hypothesis of the root cause.

Caster Breakout Near Tundish Change and Grade Separator Plate

Breakout Description

The breakout occurred on Strand 1 of 1CC's 2-strand caster. The breakout initiation location was located near 1CC's Segment 1 exit, ~6 m below the meniscus. As a result, there was a very extensive breakout shell (Fig. 2).

Further inspection of the breakout shell from Segment 1 revealed the steel strand had completely separated into two pieces along the strand width (Fig. 3a). This location was believed to be where the grade separator plates had been inserted. Fig. 3b shows an example of a separator plate used at 1CC. Initially, it had not been determined how the TC-SP contributed to the breakout event since the breakout location was so far away from mold exit. Hence, another TC-SP slab with reasonably similar grade transition (LC to HSLA) was collected and analyzed as a baseline comparison for this investigation (Fig. 3c).

There are two distinctive features on the successful TC-SP slab to note (Fig. 3c). First, there is a U-shaped grade overlap on the broad face where the incoming grade of steel overflowed onto the outgoing grade of steel in the mold. Second, there is no such overlap on the narrow face, but rather a "seam" showing the process interruption of the casting process and separation of the two steel grades.

Based on the amount and location of the breakout steel on the 1CC machine, it was suspected the breakout originated on the inner radius broad face near the north side. For this investigation, two samples were cut from the breakout slab located near the north side (Fig. 3a). These samples were deep-etched to reveal slab macrostructure,[8] and scanned using micro-x-ray fluorescence (MXRF)[8] and light-induced breakdown spectroscopy (LIBS) to measure chemical composition. Steel samples from the baseline slab at similar positions were also analyzed for comparative analysis.

Results and Discussion

Deep Etching

Steel specimens were prepared and deep-etched with copper ammonium chloride according to the procedure described by Sengupta et al.[8] Although centerline segregation was not of interest in this investigation, the etching technique has been effective to reveal crater shape macrostructure for mixed grade slabs.[2] Fig. 4 shows the macrostructures of the baseline TC-SP slab samples, which reveals the contrast between the LC (light areas)

Figure 3

Breakout shell extracted from Segment 1 of 1CC (a); example of grade separator plate inserted into mold during TC-SP (b); and slab from successful TC-SP (i.e., no breakout) for baseline comparison (c).

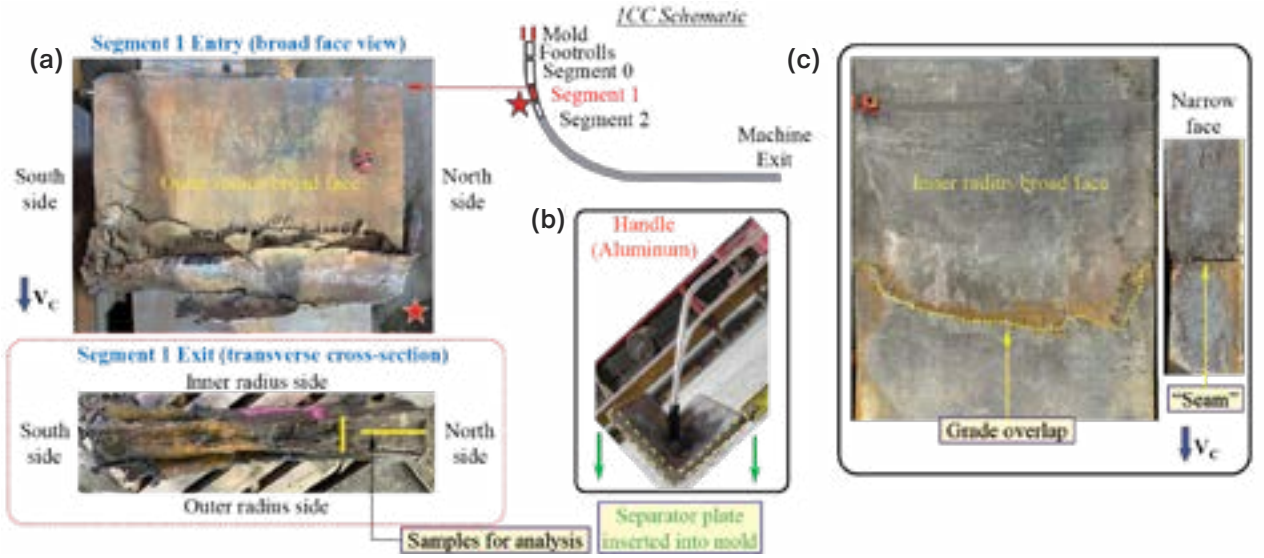

and HSLA (dark areas) and the crater shape at the time of the TC-SP. The separator plates are clearly visible in both cross-sections. In addition, steel of the outgoing grade (LC) had solidified around the separator plates prior to steel of the incoming grade (HSLA) being poured and mixing. Lastly, the grade overlap observed on the broad faces of the slab is visible in Fig. 4b as well as the "seam" on the narrow face in Fig. 4a. Along the seam and the grade overlap, there is good adhesion between the incoming and outgoing steel grades.

Fig. 5 shows the macrostructures of the breakout slab samples, which reveals the contrast between ULC (light areas) and AHSS (dark areas). There are some features similar to the baseline slab (i.e., crater shape imprint, presence of grade separator plate and solidification barrier around the plate). However, there are also features that were absent in the baseline case:

1. Cross-sections of the grade separator plates are present as well as solidification barriers of ULC that had formed around them. However, the separator plate is off-center and toward the inner radius broad face surface (Fig. 5b).

Figure 4

Deep-etched macrostructures of baseline TC-SP slab sample at broad face cross-section (a) and longitudinal cross-section (b) at mold quarter-width position.

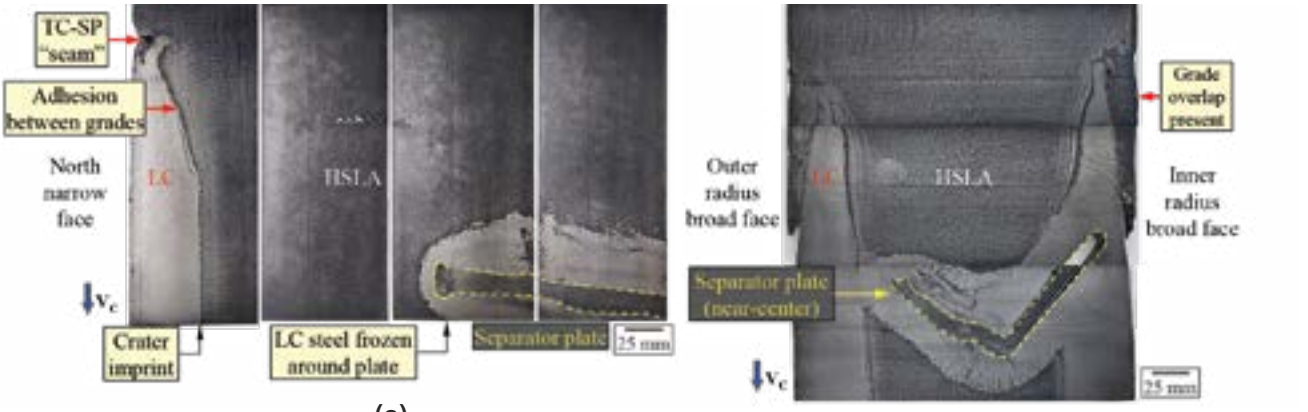

Figure 5

Deep-etched macrostructures of breakout slab removed at broad face cross-section near north narrow face of breakout slab at Segment 1 exit (a) and longitudinal cross-section at mold quarter-width location (b).

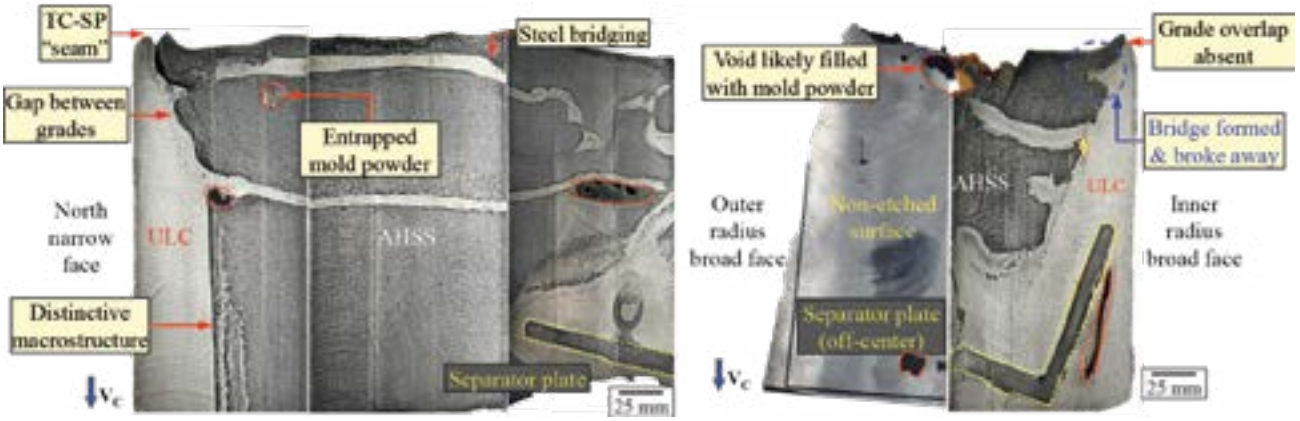

(a) (b)

2. Grade overlap, observed on the broad face surfaces of the baseline TC-SP slab, is notably absent. Furthermore, the presence of the TC-SP seam near the north narrow face (Fig. 5a) indicates the breakout originated near the TC-SP event.
3. Solidification bridges of ULC, transversing slab surfaces, are present. There are also instances of broken or short solidification bridges. It is suspected that there were bridges that had formed but broke off and washed away when new steel was poured into the mold. This is further supported by breaks in the solidification bridges observed in Fig. 5a.
4. Entrapped nonmetallic globules are present near the bridges and separator plates — later confirmed to be mold powder. Also, voids are also present in the steel, but it was likely that similar mold powder globules were present in those voids and fell out during sample preparation.
5. A distinctive macrostructure along the crater wall near the narrow face surface (Fig. 5a).
6. Separation of steel or gaps along the crater wall near the TC-SP seam between the incoming and outgoing grades.

Figure 6

Deep-etched cross-section of tail-out slab sample with examples of solidification bridging. Steel shrinkage and lack of incoming steel resulted in empty space between bridges.

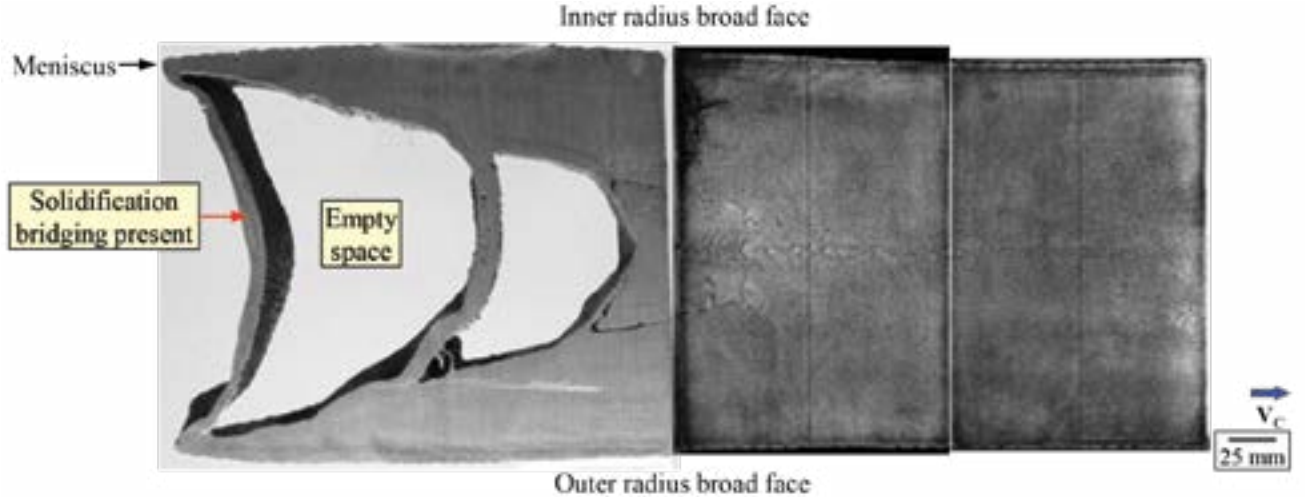

Figure 7

MXRF Mn ratio maps of baseline TC-SP slab samples superimposed onto deep-etched macrostructures from Fig. 4 along broad face cross-section (a) and longitudinal cross-section (b) at mold quarter-width position.

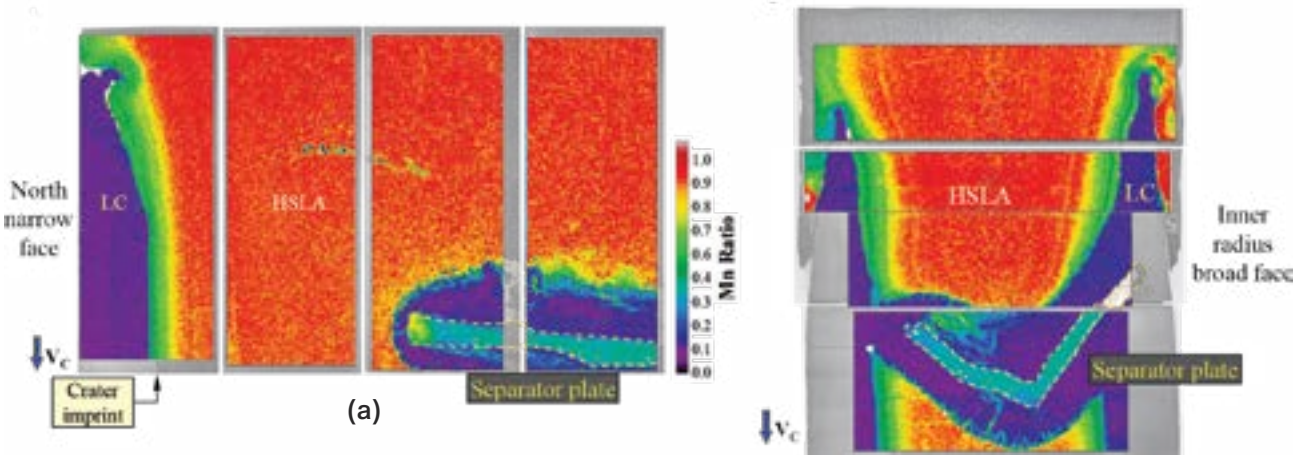

The solidification bridging phenomena had been documented once before at ArcelorMittal Dofasco during another investigation pertaining to a sequence break event and a tail-out slab. In Fig. 6, the longitudinal cross-section of the tail-out slab shows multiple layers of solidification bridges starting at the meniscus. Empty space was found to be between those bridges. During a sequence break, heat retention is reduced, owing to the absence of sufficient mold powder to provide insulation over the liquid steel. As a result, the steel at mold level is solidified. However, steel shrinkage caused by solidification along the steel strand still occurs and liquid steel is still being drawn into the crater. With no incoming liquid steel to replenish the crater, an empty space is left under the solidification bridge. This phenomenon occurred several times, creating multiple solidification bridges. The same phenomena can explain the presence of solidification bridges in the breakout slab. A long duration without new incoming liquid steel and lack of mold powder additions resulted in too much heat loss and solidification of the liquid steel surface in the mold. However, when new liquid steel was finally poured into the mold, it was able to penetrate through the bridges and fill what would have been the empty spaces.

Micro-X-Ray Fluorescence Area Scanning

The MXRF is capable of measuring manganese composition and generating large Mn area maps of steel slab samples.[2] Sengupta et al. describe the MXRF device and the Mn ratio metric which quantifies slab Mn concentration.[9–11] The slab samples in this investigation were scanned by MXRF with a 50 µm spot size and a spatial resolution of 0.5 mm.

Fig. 7 shows the MXRF Mn ratio area scans of the baseline TC-SP slab samples. Mn ratios of outgoing steel (LC) and incoming steel (HSLA) are distinct, owing to their different Mn specifications. The unique chemical composition of the grade separator plates, as well as the solidification barrier of LC steel around them, are visible. While deep-etching showed a sharp crater wall, the MXRF revealed localized grade mixing and solidification, as shown by the transitionary Mn chemistry, distinctive from both the LC and HSLA grades, which also has physical depth, as opposed to a sharp step change.

Fig. 8 shows the MXRF Mn ratio area scans of the breakout TC-SP slab samples and provides further insight into the features revealed by deep-etching. The solidification bridges that transverse slab surfaces are consistent with outgoing steel grade (ULC), indicating they had solidified prior to any grade mixing similar to the solidification barrier around the separator plates. The distinctive macrostructure by the crater wall revealed by deep-etching in Fig. 5a has a Mn ratio that is not consistent with either the outgoing or incoming steel grades, further indicating localized grade mixing. This localized grade mixing was further investigated using a different technique discussed in the next section.

Laser-Induced Breakdown Spectroscopy

With the discovery of a transitionary region of Mn ratio between the outgoing and incoming steel grades, the investigation led to the role of carbon. Despite neither grade being peritectic, it was hypothesized that a mixture of steel grades resulted in peritectic chemistry. The phenomena surrounding peritectic steels and risks associated with the continuous casting process has been well-established in literature,[12–14] but this has been for

Figure 8

MXRF Mn ratio maps of breakout slab samples superimposed onto deep-etched macrostructures from Fig. 5 along broad face cross-section (a) and longitudinal cross-section (b) at mold quarter-width position.

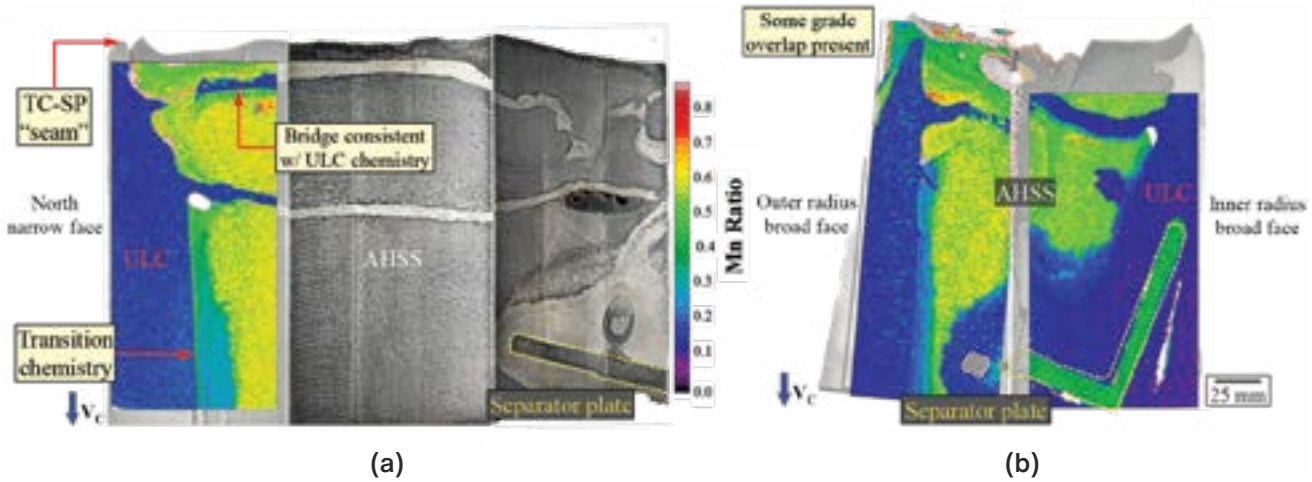

(a) (b)

Figure 9

Laser-induced breakdown spectroscopy (LIBS) analyzer (a); and LIBS "burn" marks for spot chemistry measurement (b).

(a) (b)

steady-state casting and on the steel shell solidifying along the mold wall.

The MXRF device generates high-resolution area maps of Mn composition (among other elements), but it cannot detect or measure carbon. However, LIBS is capable of detecting both carbon and manganese, but can only provide spot measurements. For this investigation, a LIBS gun measured multiple spots along the slab samples' cross-sections (Fig. 9). This article will report LIBS Mn measurements as Mn ratio — similar to the MXRF device, and carbon measurements as C-index — a normalized and unitless metric comparable to carbon wt. %. The Mn ratio profile generated by LIBS was also compared to the results generated by MXRF.

Fig. 10 shows the LIBS C-index and Mn ratio profiles for the baseline TC-SP slab and compares it to the MXRF Mn ratio profile at the same position. Mn ratio measurements between LIBS and MXRF have similar profiles and are reasonably matching. Furthermore, the C-index profile follows the Mn ratio profiles closely. C-index in the LC region closely follows C_{AIM} of the outgoing grade. C-index subsequently increases in the HSLA region within the crater and follows C_{AIM} of the incoming grade. Near the region of the crater imprint, the C and Mn measurements transition in between C_{AIM} of both grades, which is consistent with the localized mixing measured by MXRF.

Figure 10

Baseline TC-SP slab sample with LIBS measurement locations (a); and C-index and Mn ratio profiles obtained by LIBS and MXRF (b).

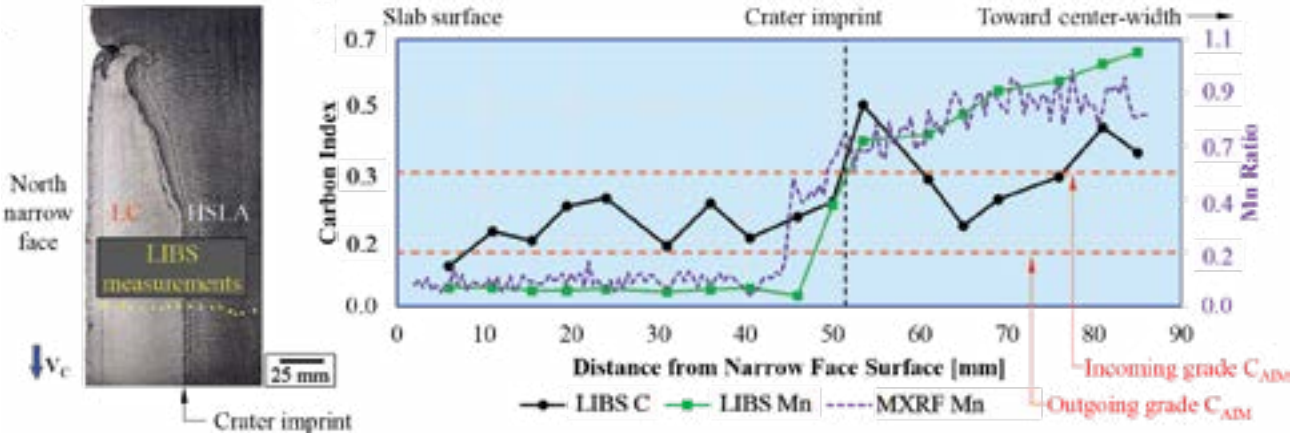

(a) (b)

Fig. 11 shows C-index and Mn ratio profiles for the breakout slab. The chemistry profiles exhibit similar behaviors to the baseline case. The distinctive macrostructure near the crater wall, which had a transition Mn ratio by MXRF, also exhibits similar behavior with respect to C-index. In fact, the transition chemistry falls within the peritectic range for C-index.

Fig. 12 shows C-index and Mn ratio profiles for the breakout slab near the initiation point. A MXRF scan of that region was not possible owing to the irregular edge. Nonetheless, LIBS Mn ratio has been demonstrated to closely match Mn ratio by MXRF. Many of the C-index measurements in the AHSS region are midway between C_{AIM} of the outgoing and incoming grades. Additionally, many of these measurements were within the peritectic range. Continuous casting of peritectic steels have been associated with wavy shell growth in the mold.[12–14] This phenomenon could also explain the separation of steel or gaps observed along the crater wall near the TC-SP seam in Fig. 11a.

Process Data Review

Despite the evidence so far, the breakout had only occurred on one of the two strands. The opposite strand

Figure 11

Breakout slab sample with LIBS measurement locations (a); and C-index and Mn ratio profiles obtained by LIBS and MXRF (b).

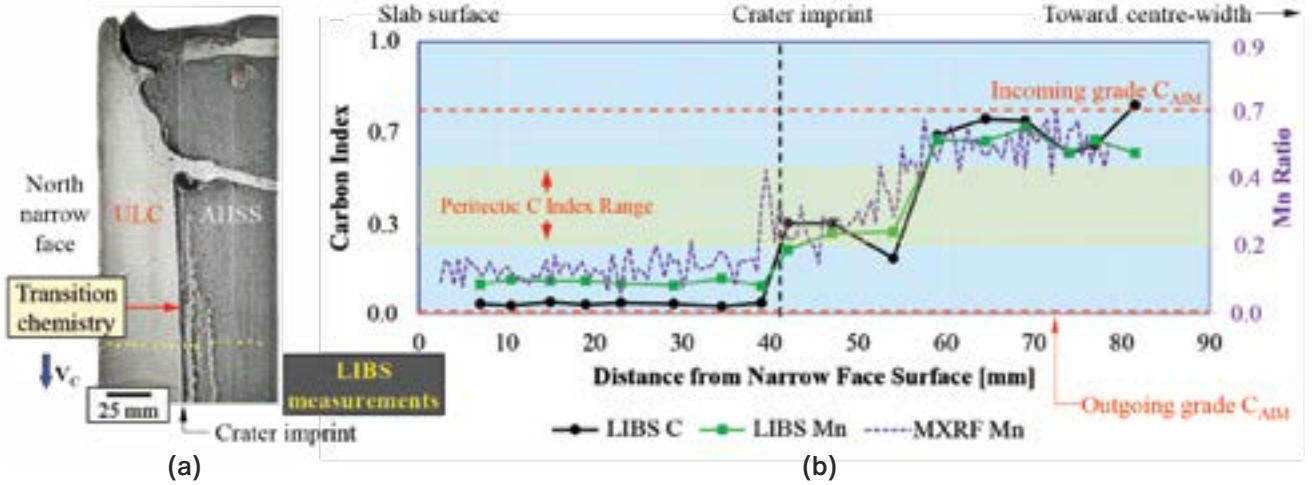

(a) (b)

Figure 12

Breakout slab sample with LIBS measurement locations (a); and C-index and Mn ratio profiles obtained by LIBS (b).

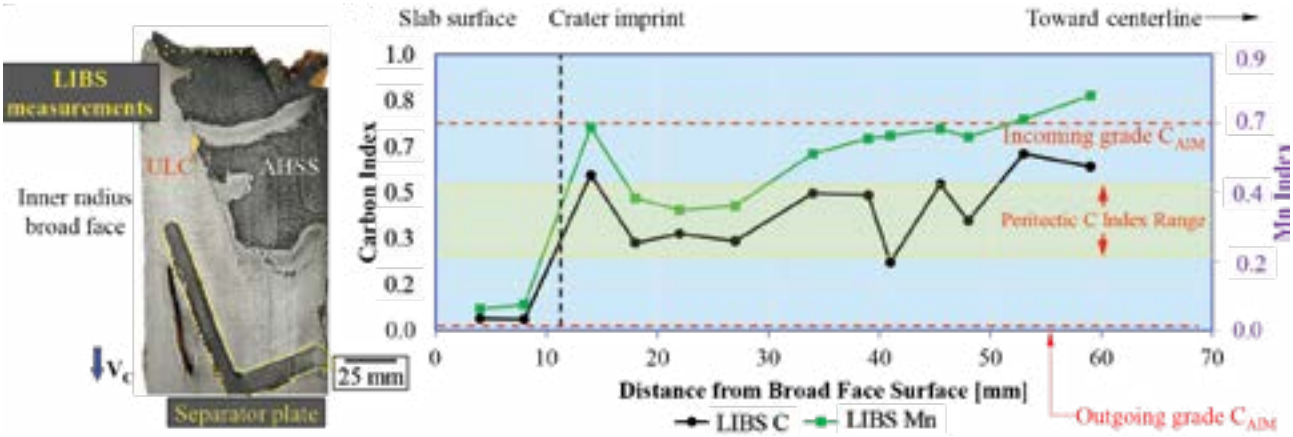

(a) (b)

did not suffer from a breakout. Furthermore, TC-SP for this specific grade transition had been successfully executed multiple times prior. Hence, the contributing factors on the strand with the breakout needed to be identified. Upon review of the process data leading up to the breakout event, further influencing factors were identified.

Fig. 13 shows key process data (cast speed [V_C] and mold width) for both strands. As per the TC-SP standard operating procedure,[2] cast speed is reduced and steel flow into the molds is cut off prior to the FTC. At very low cast speed, tundish is changed and separator plates are inserted into the molds (~2.5 minutes). Flow of liquid steel into the molds is subsequently resumed. It should be noted it took longer to resume the flow of liquid steel on the Strand 1 mold (breakout strand) compared to Strand 2, which could have resulted in the solidification bridging observed on the slab sample.

Despite this, the TC-SP section of the strand had exited the molds without any issue. However, as that steel segment traveled down the machine, the mold width on Strand 1 had been increased. Based on the distance from the breakout initiation point to the meniscus, the TC-SP section would have been traveling through 1CC's bending segment (Segment 0) during the mold width change. Immediately after the mold width change, the mold level drop was observed indicating the loss of liquid steel containment in the strand, and subsequently the breakout.

Figure 13

Process data of 1CC leading to breakout event.

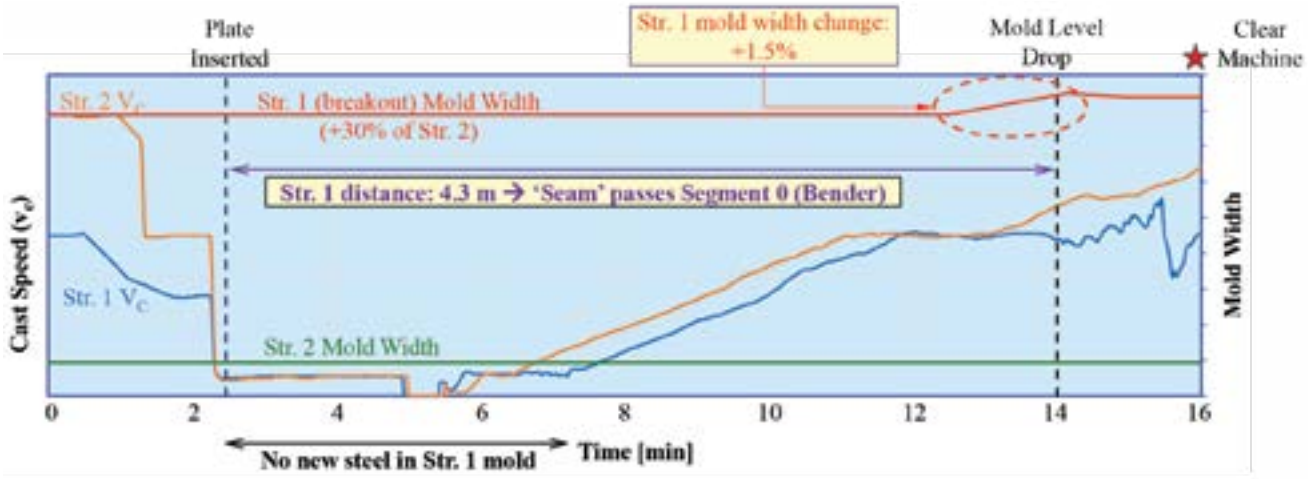

Figure 14

Schematic summary of breakout mechanism.

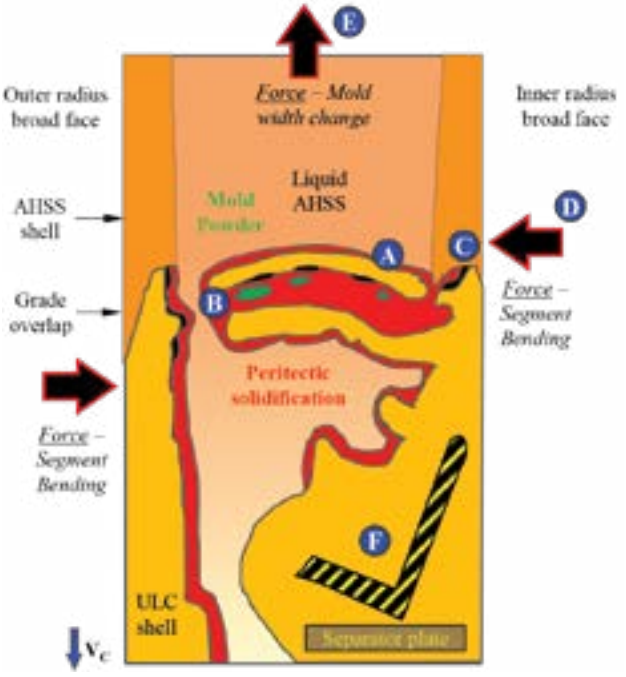

The order to "clear" the 1CC machine was given shortly after.

Breakout Mechanism

Based on the evidence provided by deep-etching, MXRF, LIBS and process data review, the contributing factors leading to the breakout event were identified. Fig. 14 shows the schematic summary of the proposed breakout mechanism.

- Integrity of the strand near the grade separator plate position (TC-SP seam) was compromised as a result of the following:
  - The long duration of no incoming steel flowing into the mold (stopper rod closed to stopper rod opened) resulted in heat loss and solidification bridging (A).
  - Solidification bridging inhibited adequate grade mixing within the strand crater.
  - Solidification bridging also resulted in more entrapped mold powder globules (B).
  - Grade mixing between ULC and AHSS grades near the TC-SP seam resulted in localized peritectic solidification near the outgoing grade steel shell and solidification bridges, creating localized regions of shrinkage and gaps between the two grades (C).
- The bending segment exerted force on the weakened TC-SP seam as it traveled through that segment (D).
- A mold width change occurring simultaneous to the TC-SP seam reaching the bending segment exerted additional force on the TC-SP seam (E).
- The grade separator plate insertion was not directly responsible for the breakout event, but rather indirectly by contributing to the longer duration of the TC-SP event (F).

Summary and Conclusions

A caster breakout occurred at ArcelorMittal Dofasco's No. 1 Continuous Caster near a TC-SP event, transitioning from ULC to AHSS. An investigation took place to identify the key contributors of the breakout event and determine the root cause. Another slab near a successful TC-SP, transitioning to LC to HSLA, was also analyzed as a baseline comparison. A failure mechanism, based on evidence from the investigation, was proposed to explain the breakout. Several conclusions are made:

1. Deep-etching, MXRF and LIBS are useful tools to characterize macrostructures and localized chemical compositions in slabs — particularly mixed-grade slabs.
2. C-index and Mn ratio profiles were similar. Carbon segregation and distribution follows very closely to that of manganese.
3. The strand section containing the grade separator plates and the TC-SP seam was structurally compromised due to long duration with no incoming steel. Despite the TC-SP seam being intact upon leaving the mold, process changes (i.e., mold width change) occurring simultaneous to the TC-SP seam traveling through the bender segment ruptured the seam and created the breakout.
4. Since this incident, ArcelorMittal Dofasco has removed the plate practice and implemented process and scheduling restrictions to prevent reoccurrence, impacting slab yield, but protecting the operators as well as the customer.
5. Caster breakouts continue to be safety and productivity risks that require investigation and discussion to improve safety in the steel industry.

Acknowledgments

The authors would like to thank their colleagues at ArcelorMittal Dofasco and Global R&D Hamilton for their support in this work.

Disclaimer

Please note that the information provided in this article is provided without warranty of any kind, express or implied, and is not a recommendation of any product, process, technique, or material, nor is it a suggestion that any product, process, technique, or material should not be used. Neither ArcelorMittal Dofasco nor any of its affiliates or employees will be liable for any damage suffered as a result of use of any information provided in this article. Use of any information in this article is entirely at the user's risk. The publication of this paper does not grant any license or other right in respect of any intellectual property owned by ArcelorMittal Dofasco or any of its related companies.

References

1. S.D. Chung, J. Sengupta and M. Afnan Alaie, "Stopper Rod Dithering Trials at ArcelorMittal Dofasco's No. 1 Continuous Caster," *Iron & Steel Technology,* Vol. 11, No. 7, 2014, pp. 77–86.
2. J. Leung and M.K. Trinh, " Investigation on Flying Tundish Change and Separation Plate Using Micro-X-Ray Fluorescence at ArcelorMittal Dofasco's No. 1 Continuous Caster," *AISTech 2021 Conference Proceedings,* 2021, pp. 1648–1656.
3. S.D. Chung, K. Delaurier, B. MacCuish and B. Cutbertson, "Mixed Grade Model Development and Implementation at Dofasco," *AISTech 2006 Conference Proceedings,* Vol. I, 2006, pp. 947–956.
4. G.N. Eaves, D.P. Stefanik and J. Neri, "Sequential Casting of Mixed Grades at Dofasco," *1991 Steelmaking Conference Proceedings,* Iron & Steel Society, pp. 729–735.
5. K. Stransky et al., "A Breakout of a Slab After Quick Changing the Tundish and Steel Quality," *METAL 2011 Proceedings,* 2011, pp. 99–104.
6. P. Rasmussen, "Mixed Grade Casting With Turbostop Impact Pads at Dofasco," *Iron and Steelmaker,* Vol. 24, No. 3, 1997, pp. 69–73.
7. J. Leung and J. Sengupta, "Wealth of Knowledge Frozen in Time: Innovative Breakout Shell Autopsy," *AISTech 2016 Conference Proceedings,* 2016, pp. 1419–1426.
8. J. Sengupta et al., "Qualitative and Quantitative Techniques for Evaluating Manganese Segregation in Advanced High-Strength Steels at ArcelorMittal Dofasco's No. 1 Continuous Caster," *AISTech 2011 Conference Proceedings,* 2011.
9. J. Sengupta, J. Leung and K. Witherspoon, "Bridging the Gap: MXRF Technique Rapidly Maps Centerline Segregation," *AISTech 2018 Conference Proceedings,* 2018, pp. 1619–1629.
10. J. Sengupta, J. Leung and A. Noorafkan, "Calibration and Validation of X-Ray Fluorescence Technique for Mapping Centerline Segregation on Steel Slabs," *AISTech 2017 Conference Proceedings,* 2017, pp. 1925–1938.
11. J. Sengupta and A. Noorafkan, "Quantifying Slab Centerline Segregation: MXRF Eliminates Sample Preparation and Etching Procedures," *AISTech 2018 Conference Proceedings,* 2018, pp. 2637–2649.
12. A. Grill and J.K. Brimacombe, "Influence of Carbon Content on Rate of Heat Extraction in the Mould of a Continuous-Casting Machine," *Ironmaking and Steelmaking,* Vol. 3, No. 2, 1976, pp. 76–79.
13. S.N. Singh and K.E. Blazek, "Heat Transfer and Skin Formation in a Continuous-Casting Mold as a Function of Steel Carbon Content," *Journal of Metals,* Vol. 26, No. 10, 1974, pp. 17–27.
14. G. Xia et al., "A Study About the Influence of Carbon Content in the Steel on the Casting Behavior," *Steel Research International,* Vol. 82, No. 3, 2011, pp. 230–236.

AISTech This paper was presented at AISTech 2025 — The Iron & Steel Technology Conference and Exposition, Nashville, Tenn., USA, and published in the AISTech 2025 Conference Proceedings.